



## Experimental Study of the Microwave Radar Doppler Spectrum Backscattered from the Sea Surface at Low Incidence Angles

M. S. Ryabkova\*, V. Yu. Karaev, Yu. A. Titchenko and E.M. Meshkov

Geophysical Research Division, Institute of Applied Physics of the Russian Academy of Sciences, Nizhny Novgorod, Russia

### Abstract

Measurements of the sea surface backscatter at low incidence angles were performed using Ka-band Doppler radars from the offshore platform in the Black Sea in October of 2016. One of the radars has a symmetrical antenna beam; the other one has a knife-like antenna beam. Incidence angles varied from nadir to 20° during experiments. In this paper the first results of experimental data processing are presented and the dependency of Doppler frequency shift, Doppler width and radar cross section on incidence angle are analyzed. Data acquired in the experiments can be used for validation of theoretical models.

### 1. Introduction

There is a significant number of theoretical studies and computation simulations of Doppler Spectrum (DS) for the case of backscattering from the sea surface at low incidence angles [1-4]. But experimental studies are not so numerous, for example, Plant *et al.* [5] investigated the dependence of microwave backscatter from the sea surface on illuminated area for X and Ka band for incidence angle of 45°. Mouche *et al.* [6] used SAR measurements for validations of different scattering models (C and Ku band, 23° and 33.5°).

Measurements of the sea surface backscatter at low incidence angles were performed using Ka-band Doppler radars from the offshore platform in the Black Sea in October of 2016. Experiments were performed for different wind speeds and wind directions, and the dependency of spectra and energy characteristics on incidence angles (0-20°) and azimuth angles (varied within the range from 0° to 140°) were studied. In this paper the first results of experimental data processing are presented and the dependency of Doppler frequency shift, Doppler spectrum width and radar cross section on incidence angle are analyzed.

### 2. Description of Experiment

Two Ka-band Doppler radars were used in the experiment, one of the radars has a knife-like antenna beam (30°x1°) and wavelength 8.9 mm (33.8 GHz) and another has a symmetrical (6°x6°) antenna beam and wavelength 8.3 mm (36.1 GHz).

The radar with a knife-like antenna beam is based on the 9 mm frequency modulated continuous wave marine radar, without determining the Doppler frequencies created by Micran [7]. Radar was developed for determining the exact distance to reflective objects. Parameters of the radar are shown in Table 1.

Table 1. Micran radar

Receiving tract input frequency range, GHz	33.4 – 34.2
Receiving tract output frequency range, MHz	0.0 – 1.4
The transmission coefficient of the receiving tract, dB	> 25
The noise factor of the receiving tract, dB	< 5
Transmitting tract input frequency range, MHz	4.175 – 4.275
Transmitting tract maximum output power, dBm	> 16
The reflection coefficient of transmitting tract for the input, dB	< -10
Currents on supply circuits, mA,	
- Plus 5 V	800
- Minus 5 V	200

In the IAP RAS the radar was upgraded to determine the Doppler frequencies with sign in a band of tens of kHz at low range resolution. Low range resolution is required to receive signals from all angles of antenna beamwidths.

The rotating apparatus was made for radar manipulations. As shown on Fig.1 the radars were placed near each other and were taking measurements simultaneously. Due to the different operating frequencies they did not influence each other's measurements. The rotating apparatus allowed changing azimuth angle by turning around Z axis (see measurement scheme on Fig. 2) and also changing incidence angle by inclining in ZY plane.

Experiment took place on the offshore platform of the Black Sea Hydrophysics Facility near the Katsiveli settlement (coordinates of the platform are 44°23'38''N, 33°59'15''W). The platform is located approximately 500 m to the south from the shore at a depth of 28 m in the open sea. The radars stood on the north corner of the platform, they were fixed at a height of 13,5 m above the sea surface. The speed and direction of the wind at a height of 5 m were measured simultaneously.

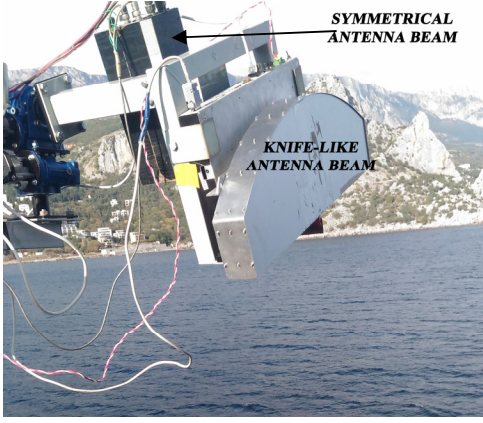


**Figure 1.** Ka-band Doppler radars

The measurement scheme is shown in Fig. 2.

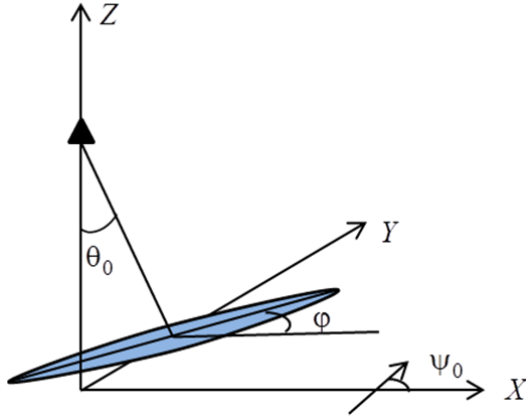


**Figure 2.** Measurement scheme

The aperture of the knife-beam antenna pattern oriented vertically downward at an incidence angle  $\theta_0$  to the vertical, which changed from  $0^\circ$  to  $20^\circ$ . X axis is pointed north, the angle between antenna major axis and the X axis is  $\phi$ . Wind direction  $\psi_0$  is measured from X axis and accounts for the direction to where the wind is blowing. Relative wind direction is calculated as  $\phi^* = \phi - \psi_0$ .

### 3. Data processing

In the quasi-specular region (the incidence angle is less than  $10 - 15^\circ$  [8, 9]), scattering occurs on the facets perpendicular to incident radiation. Motion of the "reflecting" surface segments gives rise to the Doppler shift and broadening of the DS of the signal reflected from the water surface. As a result, the DS parameters for fixed radar are completely determined by the large-scale surface characteristics (in terms of two-scale model).

We understand the DS as the power spectral density of the process, which is calculated by definition through the Fourier transform of the autocorrelation function of the process. By solving the problem of backscattering by the

surface in the Kirchhoff method approximation, Titchenko *et al.* [10] obtained the formula for the DS width  $\Delta\omega_{10}$  at the level of -10 dB relative to the maximum and for the DS shift from the carrier frequency. DS width and shift depend on the second moments that characterize sea surface state and the antenna pattern. Formulas presented in [10] can be used to theoretically calculate DS.

Here we are focusing on obtaining DS width and shift from experimental data. In case of near-nadir measurements the DS shape of the reflected signal can be approximated by Gaussian and the spectrum can be represented as follows

$$S(\omega) = A_0 \exp\left(-\frac{(\omega - \omega_{sh})^2}{4k^2\omega_s}\right) \quad (1),$$

$$\omega_s = \left(\frac{\pi^2 \Delta\omega_{10}}{4k^2}\right)^2 \frac{1}{\ln 10} \quad (2),$$

$\omega_s$  is the coefficient depending on the wave parameters and the antenna pattern.  $\Delta\omega_{10}$  is the width of DS at the level of -10dB,  $\omega_{sh}$  – Doppler frequency shift. The spectrum amplitude  $A_0$  depends on many parameters, but it is not used in further processing.

After taking the logarithm of (1), we get the following equation

$$\ln(S(\omega)) = \ln(A_0) - \frac{(\omega - \omega_{sh})^2}{4k^2\omega_s} \quad (3).$$

(3) is a linear equation for variable  $x=(\omega-\omega_{sh})^2$ . We use linear regression algorithm to get  $\omega_s$ , that allows us to calculate the DS width at the level of -10dB

$$\Delta\omega_{10} = \frac{2k\sqrt{\omega_s \ln 10}}{\pi} \quad (4).$$

We use this procedure to analyze measured DS.

### 4. Experiment results

Wind (at height of 10 m) throughout the experiment varied from 2.3 m/s up to 3.1 m/s, the azimuth angle of the antenna was stable  $\phi=142,7^\circ$  relative wind direction was changing from  $\phi^*=75.3^\circ$  to  $\phi^*=63.7^\circ$ . Doppler radar measures the backscatter intensity and the DS of the reflected signal. The DS and energy properties are shown on Fig. 3-5. An observational error of incidence angle and relative wind direction measurements is  $1^\circ$ . DS frequency shift dependency (Fig. 3) shows that at  $\theta_0=1.2^\circ$   $\omega_{sh}=0$ . Therefore  $\theta_0=1.2^\circ$  can be considered nadir, and  $\theta_0=0^\circ$  is  $\theta_0=-1.2^\circ$ .

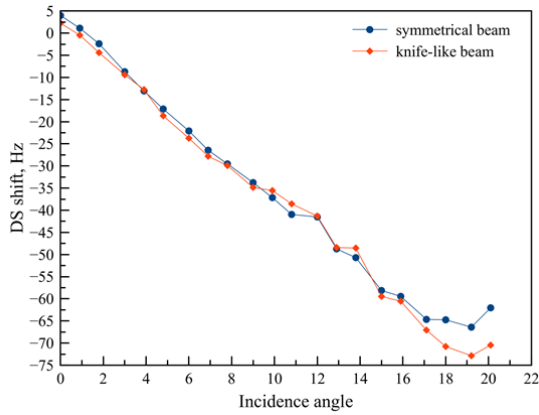


**Figure 3.** Dependency of DS shift on incidence angle

According to Kirchhoff approximation (KA) DS width should slowly decrease with increasing incidence angle (see formulas in [10]). For conditions of the experiment KA can be applied up to  $\theta_0=8^\circ$  (or  $\theta_0=7^\circ$  if  $\theta_0=1.2^\circ$  is considered nadir). After that angle DS width increase with increasing incidence angle, that shows increasing influence of Bragg scattering mechanism.

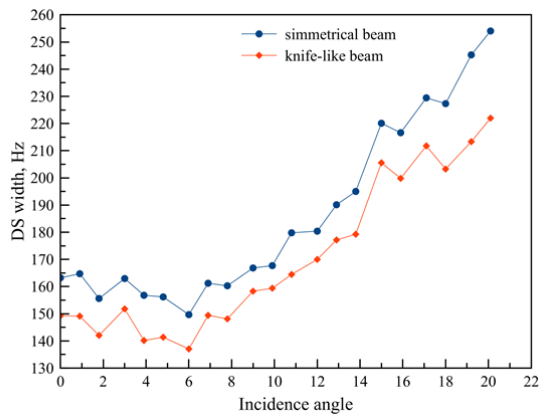


**Figure 4.** Dependency of DS width on incidence angle

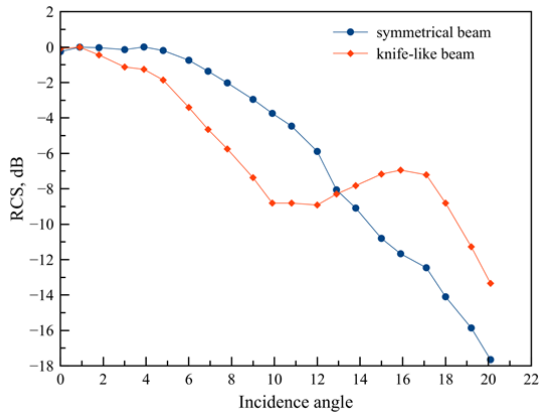


**Figure 5.** Dependency of signal power on incidence angle

The backscattering cross sections shown in the Fig. 5 have been normalized with respect to their maxima for convenience of comparison. The backscattering cross section for the antenna with a knife-like beam decline more rapidly than the backscattering cross section for the antenna with symmetrical beam due to the fact that incidence angle change in the plane along which antenna pattern is  $1^\circ$ .

Generally, experiment results are in good agreement with numerical simulations performed by Fois *et al.* [4], DS frequency shift changes its dependency in the vicinity of  $19^\circ$ . The secondary peak in signal power of the antenna with knife-like beam at  $16^\circ$  occurs due to the influence of the second sidelobe of the antenna with knife-like beam. For the antenna with symmetrical beam this effect doesn't occur due to the different antenna pattern.

## 5. Conclusions

The paper presents the first results of experimental data processing. Data were obtained during in situ observations on the offshore platform of the Black Sea Hydrophysics Facility near the Katsiveli settlement in October of 2016. Measurements of the sea surface backscatter at low incidence angles were performed using two Ka-band Doppler radars. One of the radars has a knife-like antenna beam ( $30^\circ \times 1^\circ$ ) and wavelength 8.9 mm (33.8 GHz) and another has a symmetrical ( $6^\circ \times 6^\circ$ ) antenna beam and wavelength 8.3 mm (36.1 GHz). Experiments were performed for different wind speeds and wind directions, and different wave parameters. The dependency of Doppler frequency shift, Doppler width and radar cross section on incidence angle are analyzed.

The secondary peak in signal power of the antenna of knife-like beam occurs due to the influence of antenna pattern. Data acquired in the experiments can be used for validation of theoretical models. We are planning to conduct quantity comparison of the experimental data with existing analytical models.

## 6. Acknowledgements

This work is supported by the Russian Foundation of Basic Research (grant 15-45-02501-r\_povolzhe\_a, 16-35-00548 mol\_a). Authors express their gratitude to the Black Sea Hydrophysics Facility for the access to the platform, ZAO NPF "Micran" for radar with knife-like antenna beam and the Air-sea interaction laboratory of the A.M. Obukhov Institute of Atmospheric Physics of the Russian Academy of Sciences for the wind data.

## 7. References

1. F. Nouguier, Ch.-A. Guerin and G. Soriano, "Analytical techniques for the Doppler signature of sea surfaces in the microwave regime – I: Linear surfaces,"

- IEEE Trans. Geosci. Remote Sens.*, vol. 49, no. 13, Dec. 2011, pp. 4856–4864
2. F. Nouguier, Ch.-A. Guerin and G. Soriano, “Analytical techniques for the Doppler signature of sea surfaces in the microwave regime – I: Nonlinear surfaces,” *IEEE Trans. Geosci. Remote Sens.*, vol. 49, no. 13, Dec. 2011, pp. 4920–4927
  3. J.V. Toporkkov and G.S. Brawn, “Numerical Study of the Extended Kirchhoff Approach and the Lowest Order Small Slope Approximation for Scattering from Ocean-Like Surfaces: Doppler Analysis,” *IEEE Trans. Antennas and Propagation*, vol. 50, no. 4, Apr. 2002, pp. 417-425
  4. F.Fois P. Hoogeboom, F.L. Chevalier, and A. Stoffelen, “An analytical model for the description of the full-polarimetric sea surface Doppler signature,” *J. Geophys. Res. Oceans*, vol. 120, Jan. 2015, doi: 10.1002/2014JC010589
  5. W.J.Plant, E.A.Terray, R.A.Petitt, W.C.Keller, “The dependence of microwave backscatter from the sea on illuminated area: correlation times and lengths,” *J. Geophys. Res.* vol. 49, no. C5, 1994, pp. 9705-9723
  6. Mouche, A. A., B. Chapron, N. Reul, and F. Collard, “Predicted Doppler shifts induced by ocean surface wave displacements using asymptotic electromagnetic wave scattering theories,” *Waves Random Complex Media*, vol. 18, no. 1, 2008, pp. 185–196.
  7. V.A. Khlusov, M.E. Rovkin, V.V. Dotsenko, M.V. Osipov, A.S. Surkov, D.M. Nosov, O.Y. Svarovsky, D.A. Popov, E.A. Davydenko, “LPI Ka-band radar sensor,” *CriMiCo 2012*, 2012, pp. 1090-1091
  8. G.Valenzuela, “Theories for interaction of electromagnetic and oceanic waves: A review” *Boundary Layer Meteorology*, vol. 13, 1978, pp. 61-86
  9. F.G. Bass, I.M. Fuks and D. ter Haar, “Wave scattering from statistically rough surfaces”, Pergamon, 1979, p. 540
  10. Yu.A. Titchenko, V.Yu. Karaev, M.A. Panfilova, E.M. Zuykova, E.M. Meshkov, M.V. Osipov, and V.A. Khlusov, “Experimental study of the microwave radar doppler spectrum backscattered from the sea surface at small incidence angles” *Radio and Antenna Days of the Indian Ocean*, 2015, doi: 10.1109/RADIO.2015.7323374

## 8. P.S.

If you are interested in the experimental data, feel free to contact me: m.rjabkova@gmail.com.